Integrated Electrochemical and Optical Biosensing in Organs-on-Chip

Tawade, Pratik; Mastrangeli, Massimo

DOI
10.1002/cbic.202300560

Publication date
2023

Document Version
Final published version

Published in
ChemBioChem

ChemBioChem

Review
doi.org/10.1002/cbic.202300560

Chemistry Europe
European Chemical Societies Publishing

www.chembiochem.org

Integrated Electrochemical and Optical Biosensing in Organs-on-Chip

Pratik Tawade*[a] and Massimo Mastrangeli*[a]

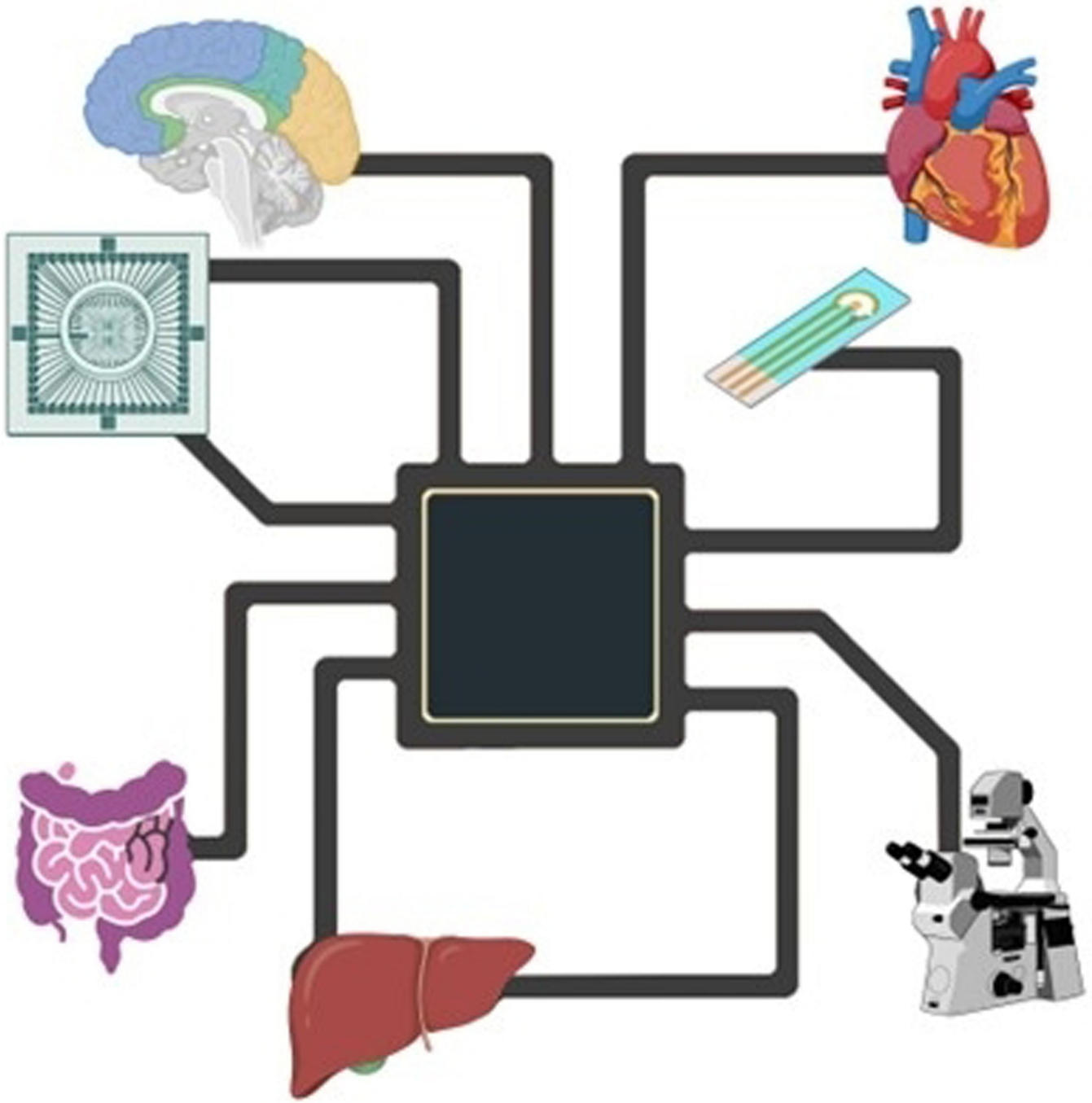

Demand for biocompatible, non-invasive, and continuous real-time monitoring of organs-on-chip has driven the development of a variety of novel sensors. However, highest accuracy and sensitivity can arguably be achieved by integrated biosensing, which enables *in situ* monitoring of the *in vitro* microenvironment and dynamic responses of tissues and miniature organs recapitulated in organs-on-chip. This paper reviews integrated electrical, electrochemical, and optical sensing methods within organ-on-chip devices and platforms. By affording precise detection of analytes and biochemical reactions, these methods expand and advance the monitoring capabilities and reproducibility of organ-on-chip technology. The integration of these sensing techniques allows a deeper understanding of organ functions, and paves the way for important applications such as drug testing, disease modeling, and personalized medicine. By consolidating recent advancements and highlighting challenges in the field, this review aims to foster further research and innovation in the integration of biosensing in organs-on-chip.

1. Introduction

For decades researchers have been dependent on *in vitro* cell cultures, let alone non-human animals, to study biological processes and the response of tissues to various therapies in pre-clinical settings. However, due to their simplistic nature, it is increasingly clear that standard cell cultures may not fully mimic the primary aspects of human physiology.[1] As they stand, *in vitro* cell cultures do not normally account for cell-matrix and cell-cell interaction, perfusion, external stimulation, and three-dimensional organization, which are conversely critical for recapitulating (patho)physiological responses. The pharmaceutical industry on the other hand routinely performs drug testing *in vivo* through organismic models based on animals, such as rodents, chimps, or pigs. Despite this, a non-negligible number of drug candidates fail in clinical trials, or even after regulatory approval and commercialization, due to serious shortcomings.[2,3] Drugs that pass pre-clinical testing in animal models may still fail to demonstrate efficacy or cause severe toxicities in humans.[4,5] Conversely, drugs and molecules potentially effective and safe in humans might not even reach clinical trials if discarded out of contradictory results in animal testing.[6] Though animal models can inherently generate systemic responses from multiple organs, which is currently difficult with conventional *in vitro* systems, eliciting and differentiating cell- or tissue-specific physiological responses therein can be hard and even lead to complications and misinterpretations. Moreover, animal models fall short of adequately representing human physiology due to important fundamental differences;[7] and ethical concerns have pushed scientists and organizations worldwide to reduce, refine, and replace (3R's) the animal models used in research.[8–10] These issues prompted the need for developing *in vitro* models more closely reproducing human physiological functions.

An organ-on-chip (OoC) is a microfluidic device containing a living engineered tissue structure, capable of recapitulating one or multiple features of the (patho)physiology of *in vivo* organs.[11] OoC models can mimic human organ responses more closely than conventional *in vitro* models. The (sub)millimetric size of OoC devices (OoCs) offers precise control of the cellular microenvironment and culture conditions and reduces the amount of cells and reagents needed, resulting in increased throughput and cost-effectiveness.[12] OoCs could be used to study onset and prognosis of diseases, discover new drugs, test their efficacy, and screen their toxicity.[13,14] There currently persists a great variance in the response toward drugs and therapies in different ethnic as well as genetic subpopulations.[15] OoC models could encode personalized biological responses accounting for genotypic variations among patients, opening to personalized medicine applications.[16]

In the early 2000s, the exploration of microfluidics to construct microphysiological systems laid the foundation for the OoC field.[17] In 2010, a groundbreaking achievement was witnessed with the demonstration of the first microfluidic devices capable of simulating specific organ functions, notably the lung-on-a-chip model. This pioneering device featured a pair of stacked microchannels vertically separated by a pneumatically-stretchable porous membrane.[18] After this milestone, focus was swiftly diversified, leading to the creation of analogous models for other organs such as gut and blood-brain-barrier (BBB).[19,20] These breakthroughs prompted studies in drug absorption, metabolism, and toxicity testing. As the field matured, the cross-talk between multiple single-organ models became a focal point to recapitulate complex interactions between diverse organs. A significant advancement was achieved in 2018 with the development of a multi-organ-on-chip (multi-OoC) system dedicated to drug metabolism research.[21] This system featured up to ten organ models coupled through integrated fluidic circuitry, facilitating the study of organ interactions in a physiologically-relevant context. Concurrently, efforts intensified towards the integration of sensors within OoC systems for real-time sensing to predict drug responses and guide personalized treatment strategies based on patient-specific reactions.[22] A representative example is the high-throughput microphysiological platform PREDICT-96.[23] This microfluidic system was designed to recapitulate hepatocyte functions under dynamic and re-circulating conditions within a 96-well microfluidic array. The latter and similar examples confirm that, to support its attractive perspectives and consolidate its reproducibility, a preeminent requirement of OoC technology lies in precise control and therefore close monitoring of the microenvironmental conditions within OoCs.

[a] *P. Tawade, Dr. M. Mastrangeli*
Electronic Components, Technology and Materials
Department of Microelectronics, Delft University of Technology
Mekelweg 4, 2628CD, Delft (Netherlands)
E-mail: p.tawade@tudelft.nl
m.mastrangeli@tudelft.nl

Accurate *in situ* measurement of biological and biochemical parameters can thereby be achieved by embedding biosensors in OoC devices and platforms.

2. Integrated Sensing in Organs-on-Chip

Much of ongoing OoC research focuses on the development of diverse organ models recapitulating human *in vivo* functionality. There consequently arises the need to monitor as well as analyse various biochemical markers and physical parameters within OoCs, as they affect cell growth, function, differentiation, and viability. Detecting biochemical, mechanical, and electrical responses to stimuli indicative of cell metabolism and function is similarly crucial. Conventional methods involve manual sample collection and off-chip analysis to characterize and evaluate cellular microenvironment, function, and organization.[24] These methods often depend on single or endpoint measurements, leading to disturbance, frequent interruption, and termination of experiments. In particular, cellular analysis and response to stimuli are usually demarcated by optical and fluorescent microscopy with the use of labelling stains, which can interact with cells and other species of interest, thereby affecting the analysis. Alternatively, OoC monitoring can be made possible by endowing OoCs with sensors.[25] Integrated and in-line sensing – ideally providing continuous, label-free, real-time sampling and analysis with minimal interference – enables sustained, reliable, and high-quality retrieval of abundant data,[26] an important and only partly met need in the OoC field.

Along with the cellular microenvironment, it is also crucial to monitor cell behaviour, which provides critical insights into cellular activity at the microscale.[27] The establishment and sustenance of concentration gradients of ions, oxygen, and biochemical species are vital for the functionality of physiologically-relevant OoCs.[28] Integrated sensors play a crucial role in spatio-temporal assessment of the effect of gradients on cell-cell and cell-matrix interactions in microphysiological systems. Uncertainty in the evaluation of such a wide range of parameters and functions of the microenvironment can lead to misinterpretation of analyses,[29] and to adverse effects on cells and tissues cultured in OoCs.[30] Hence, OoC-integrated biosensors should ideally have specific features for controlled monitoring and parameter quantification of OoCs, as summarized in Figure 1 and Table 1 which presents synoptic comparision of different sensors. The following sections provide a brief overview of integrated sensing options for OoCs.

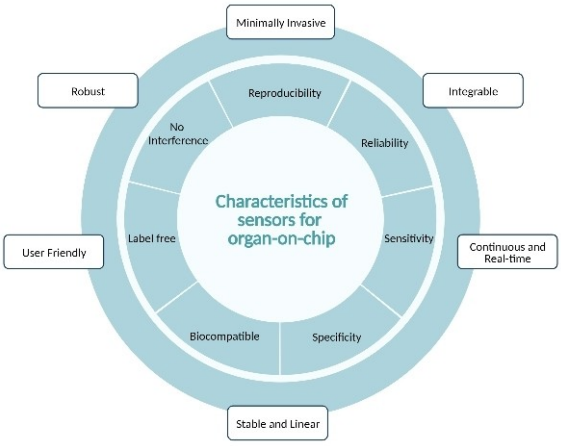

Figure 1. Characteristics of ideal sensors for OoC devices and platforms.

3. Electrical Sensing

3.1. Trans-epithelial/endothelial electrical resistance

Trans-epithelial/endothelial electrical resistance (TEER) is a crucial parameter in evaluating the epithelial/endothelial cell layer's barrier function.[31] In its basic form, TEER is measured by the voltage drop across the tissue barrier caused by an input current. TEER measurement is label-free and can be conducted continuously. The TEER value is an indicator of confluency of cells and integrity of the cell barrier, used to assess the efficacy of barriers in disease models, as well as to investigate the toxicological impact of compounds. Physiological tissue barriers have TEER values associated with their function. With TEER values varying from 1,500 to 8,000 $\Omega\,cm^2$, the blood-brain barrier is the tightest, while for the proximal conduit in the kidney TEER measures nearly 70 $\Omega\,cm^2$.[32,33]

In a standard *in vitro* transwell apparatus, the resistance across a cell layer is evaluated after physically inserting electrodes into both the upper and bottom sections of the transwell. Resistance increases as the cell membrane becomes more constrictive.[31] However, applying this method in microphysiological systems can be challenging due to the confined and

Pratik Tawade is currently pursuing his Ph.D. within the Electronic Components, Technology, and Materials group at the Microelectronics Department of Delft University of Technology. He studied Chemical Engineering at the Indian Institute of Technology Madras in India where he worked on developing microfluidic devices for drug discovery and chemical processes. His current work focuses on developing integrated sensors for organs-on-chip.

Massimo Mastrangeli is Associate Professor in the Electronic Components, Technology, and Materials group of the Department of Microelectronics of Delft University of Technology, investigating the development of innovative and scalable micro-electro-mechanical organ-on-chip devices and platforms. He is also Guest Lecturer at École Polytechnique Fédérale de Lausanne, and Board Member of the European Organ-on-Chip Society (EUROoCS).

closed nature of the devices. Additionally, compared to transwell systems, cell cultivation areas in OoCs are typically much smaller, making the exact positioning and proximity of the electrodes to the cells crucial for stable and reproducible readings. Accordingly, TEER values obtained from microfluidic devices may differ from those obtained from transwell barrier systems using the same kind of cells.[31] Integration of the electrodes in the devices can minimize the disturbances caused by manual handling.

TEER sensing electrodes have recently been incorporated into a variety of OoC models. Barrier models, including blood-brain barrier,[34] gut,[35] and lung,[36] greatly benefit from integrated TEER electrodes, typically fabricated using thin film deposition and photolithography techniques. Other applications include heart (Figure 2A)[37] and epidermis,[38] and real-time measurement of electric activity of cells during proliferation.[39] An electrode array integrated in an OoC platform for continuous TEER monitoring was fabricated using screen printing and laser processing.[40] The electrodes showed substantial stability with change in resistance of less than 0.02 Ω. An interesting opportunity lies in the integration of TEER sensing electrodes on flexible substrates, specifically for stretching tissues, as demonstrated in lung-on-chip devices.[41] TEER in OoC systems faces challenges due to lack of standardization in measurement setup and protocol, and accurate *in vivo* replication. Overcoming these issues involves optimizing cell cultures and establishing standards for operations and geometry of electrodes and tissue culture areas.

3.2. Electric cell-substrate impedance sensing

Electric cell-substrate impedance sensing (ECIS) is used to assess various aspects of cellular monolayers in OoCs. ECIS involves cultivating cells on co-planar electrodes to measure their electrical impedance at multiple frequencies. Extracted data can help evaluating cell growth and viability, spreading and attachment, morphology, motility, response to stimuli, cytotoxicity, and the healing of wounds.[42–44] ECIS can provide a qualitative analysis of variation in cellular activity and thereby differs from TEER, which mainly measures barrier function.[45]

In ECIS and similar electrode-based sensors, smaller working electrodes and a larger counter electrode with minimal impedance are typically employed because electrode impedance rises as the electrode size diminishes. Electrode arrays can obtain local impedance evaluations as a function of position. ECIS has been successfully integrated into different OoC models based on hydrogel[43] as well as polydimethylsiloxane (PDMS) (Figure 2B).[46] However, prolonged contact with cell growth medium can cause the surface of *in situ* sensor electrodes to get fouled. Frequent cleaning, shortening of experiments, or incorporation of antifouling layers are recommended to minimize fouling.[47]

3.3. Multielectrode arrays

Extracellular field potential variations result from alterations in the polarization of the cell membrane in electrogenic cells, such

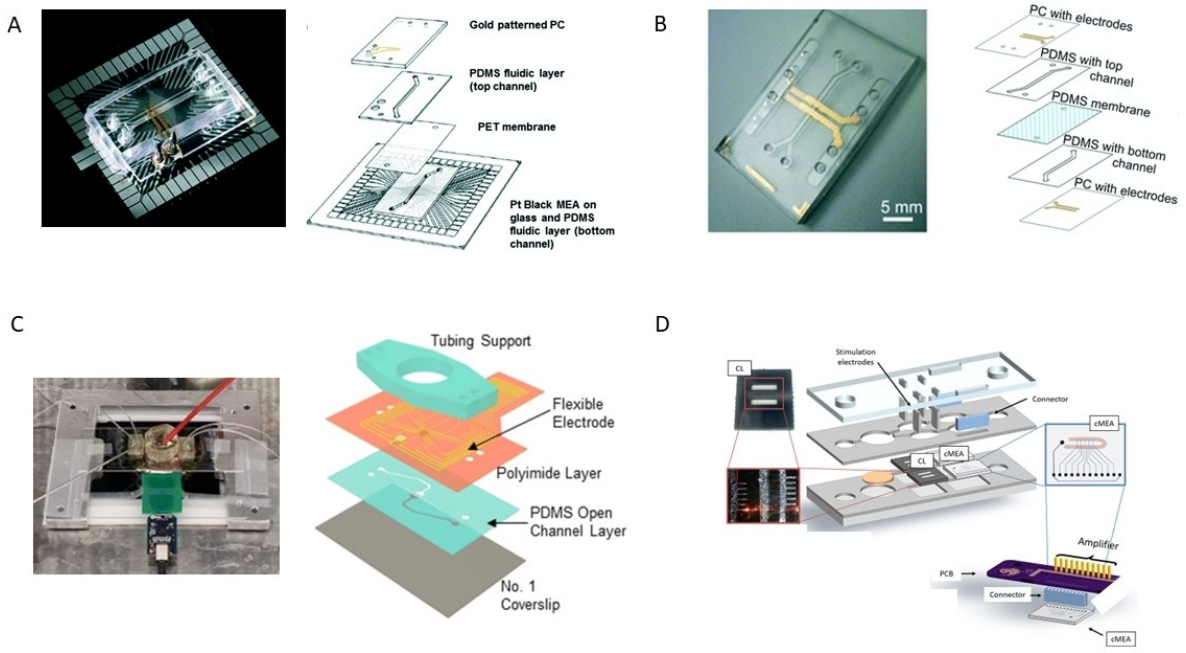

Figure 2. Examples of electrical sensors integrated on chip. (A) TEER-MEA heart-on-chip with gold TEER electrodes and platinum-black MEA. (Reprinted from[37] with permission of the Royal Society of Chemistry, 2017) (B) Microfluidic gut-on-a-chip device with patterned gold electrodes on polycarbonate substrate for TEER measurements. Reprinted from[36,46] with permission of the Royal Society of Chemistry, 2017, 2019) (C) Microfluidic chip with MEA featuring transparent graphene electrodes for retinal electrophysiological studies. (Reprinted from[52] with permission of the Royal Society of Chemistry, 2023) (D) Microfluidic multi-organ system with MEA chips (cMEA) for recording electrical signals and cantilever chips (CL) for mechanical function. (Reprinted from[56] with permission of Wiley-VCH, 2019).

as cardiomyocytes and neurons, and can be captured by voltage-sensing devices. Multielectrode arrays (MEAs) are sets of distinct (micro)electrodes that can measure the field potential of cells spatially and temporally.[48] MEAs readout can keep track of voltage peaks that appear above a predetermined threshold. MEAs have numerous applications, including models of neuromuscular junctions, heart, neuronal systems, and muscle contraction.[49] Studies of neural network processes, electro-physiological pathways linked to pathological ailments, and the impact of drugs on groups of cells are all made possible by using MEAs to detect extracellular bioelectrical potential *in vitro*. For instance, a multi-tissue-on-a-chip platform for long-term analysis was monitored using an MEA by measuring cardiac beating following exposure to drug metabolites generated by hepatic metabolism.[50,51] A recent study introduced perforated microfluidic MEAs with transparent graphene electrodes, which have the potential for chemical stimulation (Figure 2C). These MEAs were used to measure the electrical response of ganglion cells to stimulation.[52]

Within an OoC microenvironment, cells should be grown directly on the surface of MEAs to enable a high degree of spatial resolution since the electric potential reduces rapidly with distance. Both high- and low-frequency field potentials can be detected by using MEAs. Single cells exhibit a high-frequency potential, whereas linked activity among cells and total organ physiology is represented in the low frequency bandwidth (0.25–100 Hz).[53] The electrophysiological activity of cultured cells can be described by various spatiotemporal parameters, including time duration of field potential and inter-peak range.[37]

The majority of current MEAs are limited to a planar (2D) configuration, which restricts their ability to fully capture the intricate three-dimensional (3D) nature of electric tissue activity, especially within the complexities of the brain. The development and utilization of 3D MEAs are key to overcome this limitation and provide a comprehensive understanding of the signal dynamics occurring within brain tissues. To this purpose, miniature wafer-integrated MEA caps were designed to enable 3D spatiotemporal electric recording of brain organoid activity with optically-transparent shells made of self-folding polymer leaflets and conductive polymer-coated metal electrodes.[54] The authors reported a 42% increase in signal-to-noise ratio (SNR) in 3D shell electrodes compared to 2D planar ones. In another work, 3D MEAs featuring truncated Si micropyramids with vertically-arranged TiN microelectrodes were fabricated for high-throughput 3D spatial recording of neuronal tissue activity.[55] Simultaneous monitoring of mechanical and electrical cellular activity within a single chip has also been explored (Figure 2D).[56]

4. Electrochemical Sensing

An electrochemical biosensor detects biological entities by converting the information they contain into an electrical signal.[57] The principal mode of operation is the conversion of a specific biochemical reaction to an electrical output, with the purpose of recording changes in voltage or current via electrodes while simultaneously tracking biochemical responses taking place during physiological processes. Thanks to their inherent simplicity, ease of miniaturization, low prices, and outstanding analytical results, electrochemical sensors are very appealing for OoC integration.

Electrochemical biosensors with a bio-recognition element in direct contact with a transduction element lead to a permanent readout chemical reactivity which interferes with and affects the OoC microenvironment, though measurements can still be taken continuously. Numerous analytes are inactive catalysts or do not interact with catalytically-active enzymes. The detection method used in such situations is typically based on the reactions of analytes with corresponding, affinity-based enzymatic labels. It can be challenging to apply this method in continuous real-time evaluation of analytes, despite its suitability for end-point analyses. In comparison, both label- and reagent-free methods of operation are possible for potentiometric and impedimetric sensors.

Tanumihardja *et al.* measured pH and O_2 in two distinct modes using a ruthenium oxide (RuOx) electrode on-chip[58] The oxygen level was determined chrono-amperometrically, and a continuous pH measurement was acquired potentiometrically. Cardiomyocytes derived from human pluripotent stem cells were examined using RuOx electrodes to deduce two distinct metabolic processes. The pH sensor showed lower drift with 0.013 change in pH per hour and a response time of less than 2 s. An electrochemical microsensor was integrated in a breast cancer-on-chip for the detection of lactate, glucose, and oxygen.[59] A poly(2-hydroxyethyl methacrylate) (pHEMA)-based hydrogel immobilized on the electrodes measured the equimolar conversion of glucose or lactate into H_2O_2. The limit of detection for glucose and lactate sensors was reported at 7.6 μM and 6.1 μM, respectively, and less than 1 μM for oxygen sensing. A microfluidic device with a magnetic bead sensor was fabricated to detect proteins in complex culture conditions (Figure 3A).[60] A redox-labeled aptamer matching the cytokine interferon-gamma that was to be found in spiked serum was functionalized onto the beads. The square wave voltammetry output was altered by the redox label, leaving the detecting surface as a result of interferon-gamma binding. The sensitivity of this sensor (6.35 ng/ml) was claimed to be three times higher than in previous literature. The limit of detection for the optimized biosensor was reported as 6 pg/ml. To detect tiny biomarker concentrations of human cardiac troponin I (cTnI), a promising biomarker for acute myocardial infarction, a highly-sensitive microfluidic electrochemical array with miniaturized electrodes reporting a limit of detection of 5 pg/ml was produced.[61]

An integrated microfluidic device with a sensor array based on a field-effect transistor (FET) and immobilized aptamers as capture molecules was coupled with an external control system.[62] This integrated FET-biosensor platform was developed to detect cardiovascular markers in serum samples. A dual-gate FET-based charge sensor was developed by Aydogmus *et al.* and integrated into a transparent microelectromechanical OoC device (Figure 3B).[63] The overall electrode surface

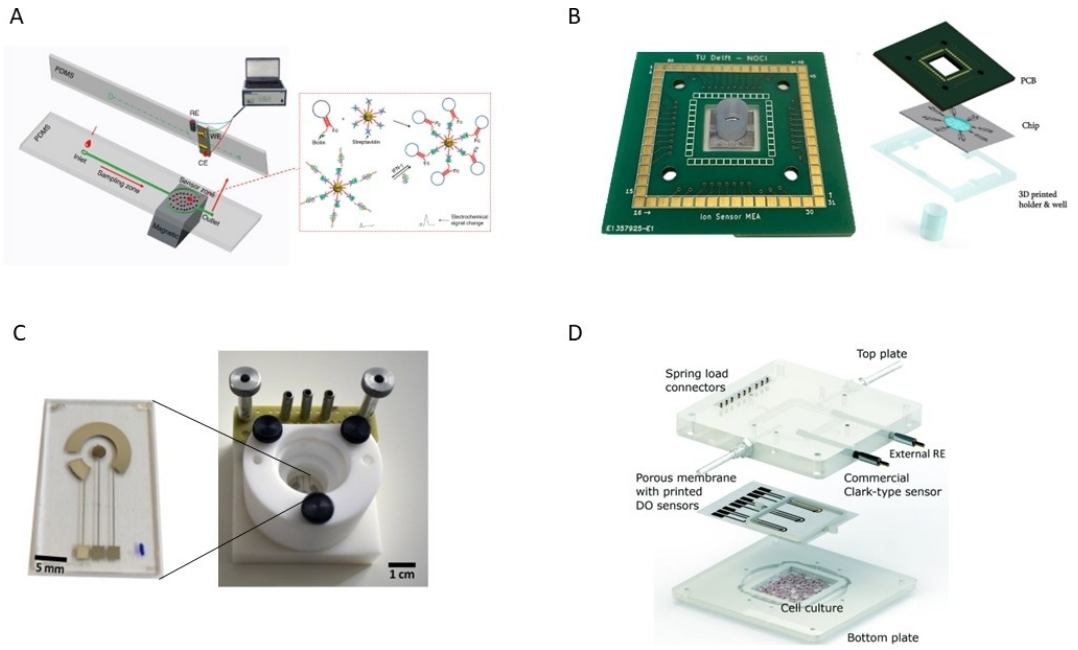

Figure 3. Electrochemical sensors integrated on chip. (A) Microfluidic device integrated with electrochemical aptamer-based sensor for monitoring of cytokines.[60] (CC BY 4.0) (B) OoC with integrated FG-FET-based pH sensor and microelectrodes for recording cellular electrical activity.[63] (CC BY 4.0) (C) Electrocatalytic RuOx-based nitric oxide sensor in an OoC. (Reprinted from[73] with permission of Elsevier, 2021) (D) Inkjet-printed electrochemical oxygen sensors in a liver-on-a-chip system. (Reprinted from[74] with permission of the Royal Society of Chemistry, 2018).

area and, consequently, sensor sensitivity were dramatically improved by the decoration of Ti-sensing electrodes with gold nanoparticle films.[64] They verified the biocompatibility of the sensor and its ability to respond to poly-D-lysine and KCl.

Potentiometric sensors, such as those based on metal oxide (MOX), ion-sensitive FETs, and organic electrochemical transistors, typically consist of an indicator electrode, the primary site for electrochemical reactions, and a reference electrode. Potentiometric sensors are used for detecting ions, including carbon dioxide, pH, and sodium ions. MOX-based sensors use manganese, zinc, or iridium as the indicator electrode and silver and silver chloride as the reference electrode.[65] The efficiency of MOX for OoC applications is supported by its quick responsiveness and resilience under extreme conditions such as extreme temperatures, humidity conditions, and harsh chemical environments.

A study demonstrated the application of a dual-sensor approach using colorimetry along with fluorescence for detecting Salmonella using ZnO-capped mesoporous silica-based nanoparticles for enhancing the biosensing in microfluidics.[66] In a different work, an electrochemical three-electrode PDMS microfluidic system with Au electrodes altered by nanosheets of CeO_2 was described.[67] This device exhibited triple enzyme mimic activity and could detect H_2O_2 released by living cells. A change in the color of the solution indicated that CeO_2 nanosheets stimulated the breakdown of H_2O_2 to generate OH^- radicals that oxidized the peroxide substrate.

Ion-sensitive (IS) membranes are used instead of indicator electrodes in FET-based sensors manufactured on silicon substrates (ISFETs). The membrane-to-reference electrode current pathway is established by applying an additional voltage. The biological receptors can be altered on their surfaces for capturing targets, and the target ions can be detected and quantified based on the transistor current. The most significant advantages of ISFETs are their compact design and tiny size, ideal for miniature systems. In organic electrochemical transistors (OECT) direct electro-chemical doping or de-doping of the conductive layer can allow the transfer of ions into active regions. By modifying the gate electrodes, OECTs have the potential to detect specific metabolism in complicated systems.[68]

Koklu *et al.* have proposed a sensor that can directly recognize glucose by eliminating the need for an additional medium.[69] They demonstrated an OECT with sideways gate electrodes modified with an enzyme and n-type compounded polymer-based channels. Flow-through continuous monitoring of glucose was enabled via microfluidic integration with increased SNR and detection limit of 1 nM. Another group showed that vertical PEDOT:PSS-based OECTs (vOECTs) improve device density and amplify the signal.[70] The spatial resolution could be increased by placing more transistors in an identified area using a vertical layout. The study demonstrated the ability of vOECTs to record concurrently both fast signals, like action potentials, and slow signals, such as multicellular potentials.

In contrast to potentiometric sensors, amperometric sensors frequently use a counter electrode as an additional electrode to safeguard the reference electrode from over-currents and maintain its half-cell potential. Amperometric sensors for OoCs should have indicator electrodes which meet the following criteria: adequate conductivity, biocompatibility, and biochemical stability against redox processes. The electrodes could be modified with biological recognizing elements. Such a techni-

que enables the sensing of non-electrochemically active species, where secondary current-responsive products could be delivered as direct inactive species.[71] Oxidase enzymes, for example, may be mounted on the indicator electrodes to facilitate the conversion of glucose to hydrogen peroxide, whose electrical signals could be monitored to detect and quantify glucose. These indirect sensors have demonstrated significant promise for assessing various electrically inactive species.[72] RuOx nanorods-based electrodes were used in an amperometric sensor for highly-sensitive and selective online monitoring of nitric oxide in OoCs (Figure 3C).[73] They showed RuOx is 115 times more selective to NO than $NaNO_2$ and reported a limit of detection of 250 mM. Moya *et al.* presented a bioreactor platform for liver-on-chip comprising an upper microfluidic chamber and a static bottom chamber (Figure 3D).[74] To measure oxygen concentrations at the inflow, middle, and outflow of the culture chamber, three amperometric electrochemical oxygen sensors were inserted in a PTFE membrane which divided the two compartments. The reported sensitivity for these sensors was 28 $nA\,L\,mg^{-1}$ and limit of detection of 0.11 $mg\,L^{-1}$ for dissolved oxygen. Electrochemical sensors in OoC systems are challenged by sensitivity to environmental conditions and real-time monitoring. Overcoming these involves adding protective coatings for durability and using specific receptor molecules to enhance selectivity.

5. Optical Sensing

Due to their high sensitivity, smooth integration with microfluidics, label-free and non-invasive operation, optical biosensors represent an appealing choice for OoC technology. These sensors pick up changes in optical absorption, illumination, refractive index, or scattering, among other optical properties. Having the ability to retrieve the signal without the sensing device making direct contact with the biological substrate is a crucial benefit of optical sensors,[75,76] enabling long-term analysis and microenvironmental monitoring without disturbing the cells. For example, Shaegh *et al.* proposed a multi-analyte optical sensor with embedded light detectors and an LED to continuously monitor oxygen and pH concentrations in a microfluidic system (Figure 4A).[77] The pH sensor showed a sensitivity of 160 mV/pH and good accuracy with a resolution of 0.03 pH, the oxygen sensor a minimum detectable variation of 0.8 % O_2 concentration. Similarly, Khalid *et al.* used optical phenol red absorbance to track pH in a lung cancer-on-chip setup which showed a sensitivity of 489 mV/pH.[78] Utilizing the intrinsic transparency of materials frequently employed in OoC manufacturing, the incorporation of optical sensors into microfluidic devices has been thoroughly investigated for real-time evaluation of analytes.[79] However, to identify specific molecules in the cell culture, some approaches would need labeled substrates; and in comparison to electrochemical systems,

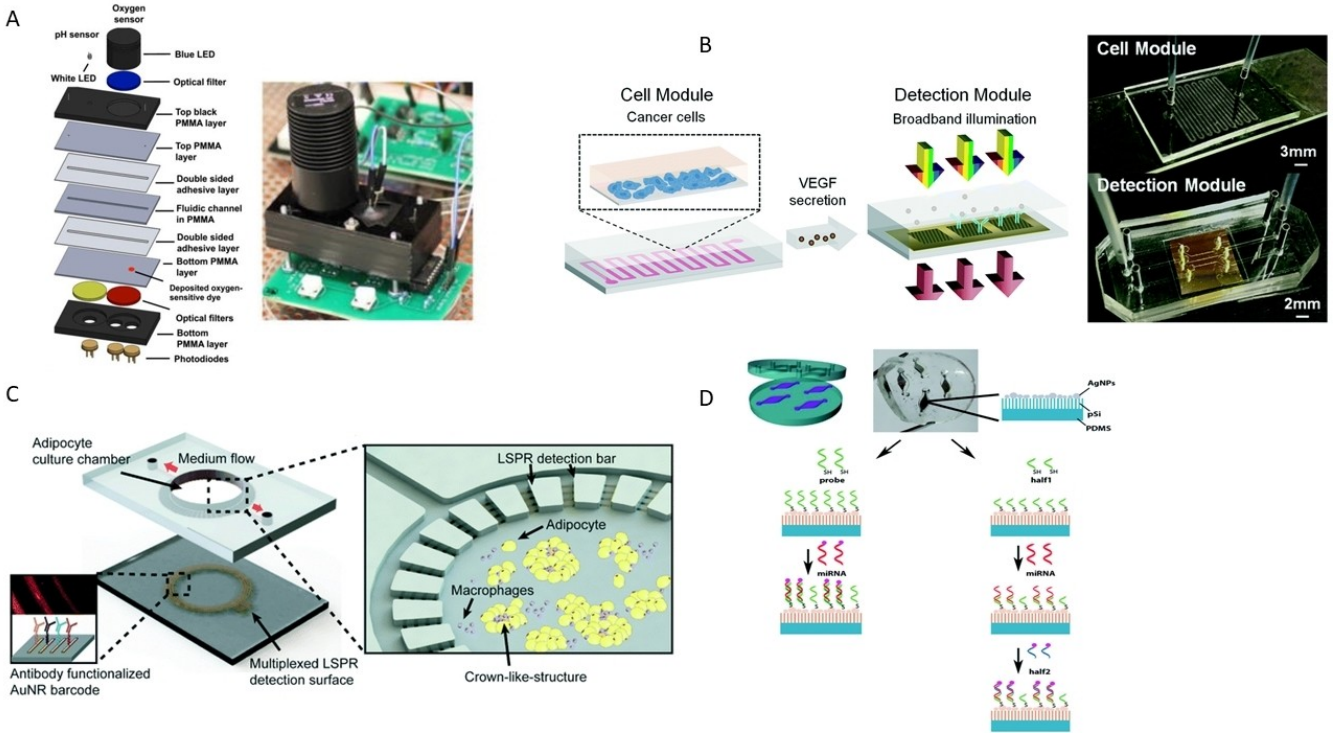

Figure 4. Examples of optical sensors combined with microfluidics. (A) Optical pH and oxygen sensor based on light absorption and quenching in an OoC. (Reprinted from[77] with the permission of AIP Publishing, 2016) (B) Plasmonic nanohole array-based biosensor for cytokine analysis in a microfluidic system. (Reprinted from[85] with permission of the Royal Society of Chemistry, 2017) (C) LSPR based optofluidic platform for sensing analytes in adipose-tissue-on-chip. (Reprinted from[98] with permission of the Royal Society of Chemistry, 2018) (D) Microfluidic platform consisting of silver-decorated porous silicon on PDMS for SERS analysis. (Reprinted from[107] with permission of the Royal Society of Chemistry, 2017).

optical instrumentation can be more expensive and sophisticated.[80]

To produce photon responses in luminescence sensors, the light source must stimulate luminescent sensing components.[81] Marker dyes are used to create or improve luminous responsiveness when compounds released during physiological processes in OoCs lack intrinsic luminescence characteristics. Dynamic quenching, which influences luminous intensity and lifetime, is a key component of oxygen sensors frequently employed in microfluidics.[82] Another option is to use an indirect sensing technique, akin to electrochemical detection. In this technique, the target analyte is converted by a biological recognition component, and an indicator dye identifies a byproduct.[83] In a perivascular niche-on-chip, Perottoni *et al.* showed a miniature system for intracellular assessment of mesenchymal stem cell activity.[84] For quantitative analysis of oxygen, they used fluorescent lifetime imaging microscopy (FLIM) with nanoparticles probe as indicator dyes.

Optical biosensors are commonly used in OoCs for protein and peptide detection. They employ biorecognition components such as antibodies and aptamers (DNA or RNA). A challenge lies in the abundance of non-specific proteins compared to the target analyte. To overcome this, a nanoplasmonic sensor was integrated in an OoC to quantitatively measure cytokine release in real time without the need for markers (Figure 4B).[85] Cytokine binding to an antibody caused a significant change in the transmitted light wavelength and showed a sensitivity of 145 pg/ml for vascular endothelial growth factor detection in complex media. Aptamer-based biosensors are also employed in OoCs due to their strong target binding and animal-free manufacturing procedures.[86] In one study, a chip-mounted aptamer biosensor targeting vascular endothelial growth factor (VEGF) was used to detect cervical cancer cells.[87] However, aptamers may be susceptible to degradation in biological fluids containing enzymes.

The ratio of transmitted and incident light intensities across an analyte with distinctive absorption peaks is the basis for absorptiometry.[88] Indicator dyes are frequently employed to interact with and change the absorption spectra of analytes lacking intrinsic spectral absorption features.[77] However, due to the proportionate correlation between attenuation and the length of the optical path, the efficacy of this detection approach is reduced in tiny reacting chambers, such as those present in microfluidic systems.

Surface plasmons (SP) are produced at the metal-dielectric interface via plasmonic resonance, which happens when light interacts with metals or other materials that have conductive electrons.[89,90] The localized changes in the adjacent medium's refractive index caused by molecules adhering to the interface affect the interfacial propagation of electromagnetic waves.[91] Metallic layers and nanoparticles are frequently used as the substrate for optical sensors because they can be incorporated into microfluidic platforms and provide superior sensitivity – as low as single-molecule level – and rich understanding without requiring labeling in biomolecular analyses.[92]

Among the most widely-used substrates for plasmon-based applications in biomedicine are aluminum, gold, and silver. The great sensitivity and stability of gold are well recognized, whereas the oxidation problems of silver are critical.[93] Additionally, due to their huge surface area-to-volume ratio and significant binding energies, 2D nanomaterials improve electromagnetic interaction on the metallic surface, amplifying the surface plasmon resonance (SPR) effect. Substrates could be nanopatterned with structures similar to or shorter than the wavelengths of light, confining surface plasmons inside the nanostructures, to further increase sensitivity in molecule recognition.[94,95]

For dynamical drug screening and cell adherence measurement, SPR-based sensing methods have been successfully coupled with *in vitro* platforms. Sensitive and label-free identification and measurement of molecules are made possible by tracing shifts in transmission spectra in real-time in OoCs. An SPR-based nanohole array, for example, was utilized in a microfluidic cellular module to identify vascular endothelial growth factor.[96] For label-free surveillance of insulin secretion, Ortega *et al.* created a biomimetic islet-on-chip system including an on-chip localized surface plasmon resonance (LSPR)-based sensing component employing modified gold nanoantennas.[97] In this study, the limit of detection of insulin was reported to be 0.85 μg/ml . Another instance is a biomimetic adipose-tissue-on-chip device that used an LSPR biosensor array made of gold nanorods coupled with an antibody to detect cytokine production from adipose tissue (Figure 4C).[98]

Lens-free imaging (LFI) is an innovative way of imaging on-chip. The foundation of LFI is the use of a coherent light source, such as a laser diode, to illuminate a specimen.[99] An image sensor is subsequently used to capture the resulting diffraction pattern. By resolving an inverse model of the light diffraction pattern, an image of the specimen can be recreated. As the name suggests, LFI eliminates the need for lenses and other costly optical elements, and allows imaging systems that are significantly compact, integrable, and affordable for a wide range of biological applications.[100] LFI is a viable option for low-cost point-of-care systems intended for resource-constrained environments, as it produces high-resolution images on a field-portable platform.[101] LFI can similarly be a viable modality for sensing in OoC systems.[102]

An effective method for detecting molecules and determining their composition, interaction, and conformity, is Raman spectroscopy.[103] Surface-Enhanced Raman Spectroscopy (SERS) considerably increases sensitivity by enhancing Raman signals using electromagnetic and chemical means. This enables quick and straightforward generation of molecular vibrational signatures and assessment of the chemical makeup of the specimens by primary analyses. The distinct spectral fingerprints of the samples can be recovered by comparison with a database of well-known chemicals. Recognition or discovery of important biochemical and structural data can thereby be enhanced by machine learning tools.

Microfluidics has benefited from the features of SERS because of its label-free, non-destructive, stable, sensitive on-chip recognition abilities, especially for trace substances.[104] Incorporating SERS in microfluidics has some clear benefits over

macroscale platforms, such as repeatable measurement settings and clearly defined detection domains.[105] Its remarkable efficacy was demonstrated in various biological substrates, including bacteria, miRNA, drugs, DNA, and food pollutants.[106–108] SERS-on-chip innovations raise further interest in personalized medicine.[109]

Metals are largely used as SERS substrates for ultra-sensitive molecule recognition by virtue of their large enhancing factor.[110] Noble metals featuring nanostructures with tailored size, symmetry, and distinct geometrical characteristics produce hotspots which significantly improve SERS.[104,111] Using DNA aptamers for interleukin 6 (IL-6) identification, Muhammad *et al.* created a structured array of gold nanoparticles as SERS substrates.[112] IL-6 was quantified in the range of 10^{-12}–10^{-7} M in serum sample with lower limit of detection of 0.8 pM. Wu *et al.* utilized silver nanocubes as hotspots for DNA detection, employing nicking endonuclease signal amplification and electrically-heated electrodes to enhance sensitivity and attain the lower limit of detection of 3.1 fM.[113] To improve SERS detection, mesoporous silica, polymeric and magnetic nanoparticles can be combined with nanostructured metal.[114] Chen *et al.* created hybrid SERS substrates by combining glycopolymers with *in situ*-produced Ag nanoparticles, displaying targeted adsorption of proteins and selective Raman amplification with minimum detection value of 10^{-7} mg/ml .[115]

In another study, a microfluidic system was created to maximize interactions among saliva specimens and a SERS substrate based on suspended Ag nanoparticles to enable quick drug detection at biologically relevant concentrations.[116] They reported presence of methamphetamine in the sample at a concentration of 10 nM, which is well below physiological value. By employing Au and Ag nanoparticles as the substrate for microfluidic technology, Kline *et al.* optimized SERS settings and claimed to attain the lowest possible limits of detection for a few drugs.[117] Other studies also included colloidal nanoparticles in media to boost detection.[118] Monitoring of intracellular SERS signals for pharmacokinetic assessment was demonstrated using a configurable microfluidic technology that used cell co-culture methods.[119] Integrated SERS systems can be advantageous for OoC applications. While high-end instruments offer optimal performance, their compatibility with compact OoC platforms is challenging. Portable Raman systems, which merge essential optical components such as miniature lasers, high-quality optics, and sensitive detectors into a compact design, may solve the issue provided sufficient accuracy and resolution. They enable real-time SERS experiments within microscale environments, providing insights into cellular processes without bulky instrumentation.[120121]

6. Summary and Outlook

This concept review presented arguments and recent highlights to foster the integration of electrical, electrochemical, and optical types of sensors in OoCs as an essential axis of research to address the field's partly unmet need for accurate and reliable monitoring. Scientists can analyze cell-specific outcomes, biochemical alterations, and disease models by incorporating non-invasive sensing modalities into OoC devices and platforms, yielding important insights into the aetiology of pathologies and enabling tailored treatment methods. As OoC technology progresses, integrated sensing will turn into an essential instrument for expanding our knowledge of human biology and hastening the development of drugs, both conducive to beneficial outcomes for patients.

Before deciding which sensor to incorporate, it is crucial to thoroughly weigh advantages and limits of each sensor type. The preferable option may depend on a number of factors, including sensing mechanism, sensitivity, selectivity, sizes and interfaces, compatibility with OoC substrates and other sensors, and sensor performance. Further research is required to increase sensitivity and selectivity, improve sensor design, and ease integration within OoCs. Furthermore, the inclusion of machine learning techniques could improve and automate the ability of OoC systems to extract, compress, and analyze data, and anticipate physiological responses in real-time.

Future research should additionally concentrate on multiplexing biomarker detection to suit the expanding trend of multi-OoC devices. The target would be a single multi-sensor system with automatic biochemical and physical detection capabilities as well as regulated stimulation. Multi-sensory platforms should be tailored to accommodate the various needs and characteristics of OoC models. Though attractive, integrating various sensing modalities in OoC devices still presents challenges. One key issue is interference between sensors in confined spaces, impacting data accuracy. The latter can be mitigated by signal processing and machine learning algorithms which enhance signal differentiation from various modalities. Additionally, diverse operational requirements pose difficulties. For instance, aligning parameters for different sensors, such as voltage and current, is crucial but can be problematic due to inherent differences. Advanced microfabrication is often employed to integrate sensors precisely in OoC devices. Micro- and nanoscale engineering solutions can help minimize interference and optimize space utilization. Standardization efforts should contribute to establish shared protocols for measurement procedures and setups, reinforcing reliability and reproducibility of results. To address customization, breakdowns, and biofouling, the design of modular and adaptable sensing platforms allowing plug-and-play and smooth sensor substitution is highly beneficial.[122] Such platforms offer the advantage of simplicity while affording the flexibility to incorporate OoC elements according to needs. Further developments should ultimately define total analysis systems for OoCs, making them affordable, user-friendly, robust, and versatile by integrating multiple sensing modalities.

Acknowledgements

This publication is part of the LymphChip project with project number NWA-ORC 2019 1292.19.019 of the NWA research program 'Research on Routes by Consortia (ORC)', which is

funded by the Netherlands Organization for Scientific Research (NWO). Figures were designed with Biorender (Biorender.com).

Conflict of Interests

The authors declare no conflict of interest.

Keywords: biosensorsorgan-on-chip · electrochemical sensors · microphysiological systems · optical sensors

[1] N. Gaio, B. van Meer, W. Quiros Solano, L. Bergers, A. van de Stolpe, C. Mummery, P. M. Sarro, R. Dekker, *Micromachines* **2016**, *7*.
[2] A. D. van der Meer, A. van den Berg, *Integr. Biol.* **2012**, *4*, 461–470.
[3] M. H. Wu, S. B. Huang, G. B. Lee, *Lab Chip* **2010**, *10*, 939–956.
[4] R. Barrile, A. D. van der Meer, H. Park, J. P. Fraser, D. Simic, F. Teng, D. Conegliano, J. Nguyen, A. Jain, M. Zhou, K. Karalis, D. E. Ingber, G. A. Hamilton, M. A. Otieno, *Clin. Pharmacol. Ther.* **2018**, *104*, 1240–1248.
[5] H. Golding, S. Khurana, M. Zaitseva, *Cold Spring Harbor Perspect. Biol.* **2018**, *10*.
[6] G. A. Van Norman, *JACC Basic Transl Sci* **2020**, *5*, 387–397.
[7] N. Shanks, R. Greek, J. Greek, *Philos Ethics Humanit Med* **2009**, *4*, 2.
[8] P. A. Ward, R. J. Blanchard, V. Bolivar, M. J> Brown, F. Chang, J. P. Herman, R. Hubrecht, D. M. Lawson, S. F. Maier, D. Morton, S. M. Niemi, M. Novak, S. L. Zawistowski in *Recognition and Alleviation of Distress in Laboratory Animals*, Washington (DC), **2008**.
[9] R. Franco, A. Cedazo-Minguez, *Front. Pharmacol.* **2014**, *5*, 146.
[10] J. Seok, H. S. Warren, A. G. Cuenca, M. N. Mindrinos, H. V. Baker, W. Xu, D. R. Richards, G. P. McDonald-Smith, H. Gao, L. Hennessy, C. C. Finnerty, C. M. Lopez, S. Honari, E. E. Moore, J. P. Minei, J. Cuschieri, P. E. Bankey, J. L. Johnson, J. Sperry, A. B. Nathens, T. R. Billiar, M. A. West, M. G. Jeschke, M. B. Klein, R. L. Gamelli, N. S. Gibran, B. H. Brownstein, C. Miller-Graziano, S. E. Calvano, P. H. Mason, J. P. Cobb, L. G. Rahme, S. F. Lowry, R. V. Maier, L. L. Moldawer, D. N. Herndon, R. W. Davis, W. Xiao, R. G. Tompkins, *Proc. Natl. Acad. Sci. USA* **2013**, *110*, 3507–3512.
[11] M. Mastrangeli, S. Millet, T. Orchid Partners, J. Van den Eijnden-van Raaij, *ALTEX* **2019**, *36*, 650–668.
[12] A. Agarwal, J. A. Goss, A. Cho, M. L. McCain, K. K. Parker, *Lab Chip* **2013**, *13*, 3599–3608.
[13] S. Adler, D. Basketter, S. Creton, O. Pelkonen, J. van Benthem, V. Zuang, K. E. Andersen, A. Angers-Loustau, A. Aptula, A. Bal-Price, E. Benfenati, U. Bernauer, J. Bessems, F. Y. Bois, A. Boobis, E. Brandon, S. Bremer, T. Broschard, S. Casati, S. Coecke, R. Corvi, M. Cronin, G. Daston, W. Dekant, S. Felter, E. Grignard, U. Gundert-Remy, T. Heinonen, I. Kimber, J. Kleinjans, H. Komulainen, R. Kreiling, J. Kreysa, S. B. Leite, G. Loizou, G. Maxwell, P. Mazzatorta, S. Munn, S. Pfuhler, P. Phrakonkham, A. Piersma, A. Poth, P. Prieto, G. Repetto, V. Rogiers, G. Schoeters, M. Schwarz, R. Serafimova, H. Tahti, E. Testai, J. van Delft, H. van Loveren, M. Vinken, A. Worth, J. M. Zaldivar, *Arch. Toxicol.* **2011**, *85*, 367–485.
[14] D. Huh, G. A. Hamilton, D. E. Ingber, *Trends Cell Biol.* **2011**, *21*, 745–754.
[15] D. B. Fogel, *Contemp Clin Trials Commun* **2018**, *11*, 156–164.
[16] A. D. Ebert, P. Liang, J. C. Wu, *J. Cardiovasc. Pharmacol.* **2012**, *60*, 408–416.
[17] G. M. Whitesides, *Nature* **2006**, *442*, 368–373.
[18] D. Huh, B. D. Matthews, A. Mammoto, M. Montoya-Zavala, H. Y. Hsin, D. E. Ingber, *Science* **2010**, *328*, 1662–1668.
[19] H. J. Kim, D. Huh, G. Hamilton, D. E. Ingber, *Lab Chip* **2012**, *12*, 2165–2174.
[20] J. A. Brown, V. Pensabene, D. A. Markov, V. Allwardt, M. D. Neely, M. J. Shi, C. M. Britt, O. S. Hoilett, Q. Yang, B. M. Brewer, P. C. Samson, L. J. McCawley, J. M. May, D. J. Webb, D. Y. Li, A. B. Bowman, R. S. Reiserer, J. P. Wikswo, *Biomicrofluidics* **2015**, *9*.
[21] C. D. Edington, W. L. K. Chen, E. Geishecker, T. Kassis, L. R. Soenksen, B. M. Bhushan, D. Freake, J. Kirschner, C. Maass, N. Tsamandouras, J. Valdez, C. D. Cook, T. Parent, S. Snyder, J. J. Yu, E. Suter, M. Shockley, J. Velazquez, J. J. Velazquez, L. Stockdale, J. P. Papps, I. Lee, N. Vann, M. Gamboa, M. E. LaBarge, Z. Zhong, X. Wang, L. A. Boyer, D. A. Lauffenburger, R. L. Carrier, C. Communal, S. R. Tannenbaum, C. L. Stokes, D. J. Hughes, G. Rohatgi, D. L. Trumper, M. Cirit, L. G. Griffith, *Sci. Rep.* **2018**, *8*.
[22] S. Fuchs, S. Johansson, A. O. Tjell, G. Werr, T. Mayr, M. Tenje, *ACS Biomater. Sci. Eng.* **2021**, *7*, 2926–2948.
[23] K. Tan, J. Coppeta, H. Azizgolshani, B. C. Isenberg, P. M. Keegan, B. P. Cain, A. J. Patterson, E. S. Kim, L. B. Kratchman, M. Rogers, N. Haroutunian, V. Newlin, S. Golmon, V. Tandon, M. J. Lu, J. R. Gosset, E. M. Vedula, J. L. Charest, S. S. Bale, *Lab Chip* **2020**, *20*, 3653–3653.
[24] M. Rothbauer, P. Ertl, *Adv. Biochem. Eng./Biotechnol.* **2020**, *179*, 343–354.
[25] A. Khademhosseini, R. Langer, *Nat. Protoc.* **2016**, *11*, 1775–1781.
[26] S. R. A. Kratz, G. Holl, P. Schuller, P. Ertl, M. Rothbauer, *Biosensors* **2019**, *9*.
[27] T. Kilic, F. Navaee, F. Stradolini, P. Renaud, S. Carrara, *Microphysiological Systems* **2018**, *2*.
[28] M. B. Furie, G. J. Randolph, *Am. J. Pathol.* **1995**, *146*, 1287–1301.
[29] G. A. Clarke, B. X. Hartse, A. E. Niaraki Asli, M. Taghavimehr, N. Hashemi, M. Abbasi Shirsavar, R. Montazami, N. Alimoradi, V. Nasirian, L. J. Ouedraogo, N. N. Hashemi, *Sensors* **2021**, *21*.
[30] G. Luka, A. Ahmadi, H. Najjaran, E. Alocilja, M. DeRosa, K. Wolthers, A. Malki, H. Aziz, A. Althani, M. Hoorfar, *Sensors* **2015**, *15*, 30011–30031.
[31] B. Srinivasan, A. R. Kolli, M. B. Esch, H. E. Abaci, M. L. Shuler, J. J. Hickman, *J Lab Autom* **2015**, *20*, 107–126.
[32] C. D. A. Brown, R. Sayer, A. S. Windass, I. S. Haslam, M. E. De Broe, P. C. D'Haese, A. Verhulst, *Toxicol. Appl. Pharmacol.* **2008**, *233*, 428–438.
[33] A. Wolff, M. Antfolk, B. Brodin, M. Tenje, *J Pharm Sci-Us* **2015**, *104*, 2727–2746.
[34] R. Booth, H. Kim, *Lab Chip* **2012**, *12*, 1784–1792.
[35] F. R. Walter, S. Valkai, A. Kincses, A. Petnehazi, T. Czeller, S. Veszelka, P. Ormos, M. A. Deli, A. Der, *Sens. Actuators B* **2016**, *222*, 1209–1219.
[36] O. Y. F. Henry, R. Villenave, M. J. Cronce, W. D. Leineweber, M. A. Benz, D. E. Ingber, *Lab Chip* **2017**, *17*, 2264–2271.
[37] B. M. Maoz, A. Herland, O. Y. F. Henry, W. D. Leineweber, M. Yadid, J. Doyle, R. Mannix, V. J. Kujala, E. A. FitzGerald, K. K. Parker, D. E. Ingber, *Lab Chip* **2017**, *17*, 2294–2302.
[38] F. A. Alexander, S. Eggert, J. Wiest, *Genes-Basel* **2018**, *9*.
[39] J. Liu, W. Zhao, M. Qin, X. Luan, Y. Li, Y. Zhao, C. Huang, L. Zhang, M. Li, *Analyst* **2023**, *148*, 516–524.
[40] A. Krishnakumar, S. Kadian, U. Heredia Rivera, S. Chittiboyina, S. A. Lelievre, R. Rahimi, *ACS Biomater. Sci. Eng.* **2023**, *9*, 1620–1628.
[41] Y. Mermoud, M. Felder, J. D. Stucki, A. O. Stucki, O. T. Guenat, *Sens. Actuators B* **2018**, *255*, 3647–3653.
[42] Y. C. Xu, X. W. Xie, Y. Duan, L. Wang, Z. Cheng, J. Cheng, *Biosens. Bioelectron.* **2016**, *77*, 824–836.
[43] T. B. Tran, S. Cho, J. Min, *Biosens. Bioelectron.* **2013**, *50*, 453–459.
[44] L. D. Robilliard, J. Yu, S. M. Jun, A. Anchan, G. Finlay, C. E. Angel, E. S. Graham, *Biosensors* **2021**, *11*.
[45] Y. An, T. Y. Jin, F. Zhang, P. He, *J. Electroanal. Chem.* **2019**, *834*, 180–186.
[46] M. W. van der Helm, O. Y. F. Henry, A. Bein, T. Hamkins-Indik, M. J. Cronce, W. D. Leineweber, M. Odijk, A. D. van der Meer, J. C. T. Eijkel, D. E. Ingber, A. van den Berg, L. I. Segerink, *Lab Chip* **2019**, *19*, 452–463.
[47] S. C. Lange, E. van Andel, M. M. J. Smulders, H. Zuilhof, *Langmuir* **2016**, *32*, 10199–10205.
[48] P. R. F. Rocha, P. Schlett, U. Kintzel, V. Mailander, L. K. J. Vandamme, G. Zeck, H. L. Gomes, F. Biscarini, D. M. de Leeuw, *Sci. Rep.* **2016**, *6*.
[49] C. M. Leung, P. de Haan, K. Ronaldson-Bouchard, G. A. Kim, J. Ko, H. S. Rho, Z. Chen, P. Habibovic, N. Li Jeon, S. Takayama, M. L. Shuler, G. Vunjak-Novakovic, O. Frey, E. Verpoorte, Y. C. Toh, *Nat Rev Method Prime* **2022**, *2*.
[50] C. Oleaga, A. Riu, S. Rothemund, A. Lavado, C. W. McAleer, C. J. Long, K. Persaud, N. S. Narasimhan, M. Tran, J. Roles, C. A. Carmona-Moran, T. Sasserath, D. H. Elbrecht, L. Kumanchik, L. R. Bridges, C. Martin, M. T. Schnepper, G. Ekman, M. Jackson, Y. I. Wang, R. Note, J. Langer, S. Teissier, J. J. Hickman, *Biomaterials* **2018**, *182*, 176–190.
[51] C. Oleaga, C. Bernabini, A. S. T. Smith, B. Srinivasan, M. Jackson, W. McLamb, V. Platt, R. Bridges, Y. Q. Cai, N. Santhanam, B. Berry, S. Najjar, N. Akanda, X. F. Guo, C. Martin, G. Ekman, M. B. Esch, J. Langer, G. Ouedraogo, J. Cotovio, L. Breton, M. L. Shuler, J. J. Hickman, *Sci. Rep.* **2016**, *6*.
[52] A. Esteban-Linares, X. Zhang, H. H. Lee, M. L. Risner, S. M. Weiss, Y. Q. Xu, E. Levine, D. Li, *Lab Chip* **2023**, **23**, **2193-2205**.
[53] D. A. Koutsouras, R. Perrier, A. V. Marquez, A. Pirog, E. Pedraza, E. Cloutet, S. Renaud, M. Raoux, G. G. Malliaras, J. C. Lang, *Mat Sci Eng C–Mater* **2017**, *81*, 84–89.
[54] Q. Huang, B. Tang, J. C. Romero, Y. Yang, S. K. Elsayed, G. Pahapale, T. J. Lee, I. E. Morales Pantoja, F. Han, C. Berlinicke, T. Xiang, M. Solazzo, T.

Hartung, Z. Qin, B. S. Caffo, L. Smirnova, D. H. Gracias, *Sci. Adv.* **2022**, *8*, eabq5031.
[55] N. Revyn, M. H. Y. Hu, J. P. M. S. Frimat, B. De Wagenaar, A. M. J. M. Van den Maagdenberg, P. M. Sarro, M. Mastrangeli, *Proc. Ieee Micr. Elect.* **2022**, 102–105.
[56] C. Oleaga, A. Lavado, A. Riu, S. Rothemund, C. A. Carmona-Moran, K. Persaud, A. Yurko, J. Lear, N. S. Narasimhan, C. J. Long, F. Sommerhage, L. R. Bridges, Y. Q. Cai, C. Martin, M. T. Schnepper, A. Goswami, R. Note, J. Langer, S. Teissier, J. Cotovio, J. J. Hickman, *Adv. Funct. Mater.* **2019**, *29*.
[57] R. Ahmad, M. Khan, P. Mishra, N. Jahan, M. A. Ahsan, I. Ahmad, M. R. Khan, Y. Watanabe, M. A. Syed, H. Furukawa, A. Khosla, *J. Electrochem. Soc.* **2021**, *168*.
[58] E. Tanumihardja, W. Olthuis, A. van den Berg, *Sensors* **2018**, *18*.
[59] J. Dornhof, J. Kieninger, H. Muralidharan, J. Maurer, G. A. Urban, A. Weltin, *Lab Chip* **2022**, *22*, 225–239.
[60] G. Liu, C. Cao, S. Ni, S. Feng, H. Wei, *Microsyst Nanoeng* **2019**, *5*, 35.
[61] Y. Li, S. H. Zuo, L. Q. Ding, P. P. Xu, K. Wang, Y. C. Liu, J. M. Li, C. Liu, *Anal. Bioanal. Chem.* **2020**, *412*, 8325–8338.
[62] A. Sinha, T. Y. Tai, K. H. Li, P. Gopinathan, Y. D. Chung, I. Sarangadharan, H. P. Ma, P. C. Huang, S. C. Shiesh, Y. L. Wang, G. B. Lee, *Biosens. Bioelectron.* **2019**, *129*, 155–163.
[63] H. Aydogmus, M. Hu, L. Ivancevic, J. P. Frimat, A. van den Maagdenberg, P. M. Sarro, M. Mastrangeli, *Sci. Rep.* **2023**, *13*, 8062.
[64] H. Avdogmus, H. J. van Ginkel, A. D. Galiti, M. Hu, J. P. Frimat, A. Van Den Maagdenberg, G. Q. Zhang, M. Mastrangeli, P. M. Sarro, *Int Sol St Sen Act M* **2021**, 180–183.
[65] L. Manjakkal, D. Szwagierczak, R. Dahiya, *Prog. Mater. Sci.* **2020**, *109*.
[66] F. C. Huang, R. Y. Guo, L. Xue, G. Z. Cai, S. Y. Wang, Y. B. Li, M. Liao, M. H. Wang, J. H. Lin, *Sens. Actuators B* **2020**, *312*.
[67] N. Alizadeh, A. Salimi, T. K. Sham, P. Bazylewski, G. Fanchini, *ACS Omega* **2020**, *5*, 11883–11894.
[68] A. Marks, S. Griggs, N. Gasparini, M. Moser, *Adv. Mater. Interfaces* **2022**, *9*.
[69] A. Koklu, D. Ohayon, S. Wustoni, A. Hama, X. X. Chen, I. McCulloch, S. Inal, *Sens. Actuators B* **2021**, *329*.
[70] M. Abarkan, A. Pirog, D. Mafilaza, G. Pathak, G. N'Kaoua, E. Puginier, R. O'Connor, M. Raoux, M. J. Donahue, S. Renaud, J. Lang, *Adv. Sci.* **2022**, *9*.
[71] N. J. Ronkainen, H. B. Halsall, W. R. Heineman, *Chem. Soc. Rev.* **2010**, *39*, 1747–1763.
[72] D. Bavli, S. Prill, E. Ezra, G. Levy, M. Cohen, M. Vinken, J. Vanfleteren, M. Jaeger, Y. Nahmias, *P Natl Acad Sci USA* **2016**, *113*, E2231–E2240.
[73] E. Tanumihardja, A. P. Rodriguez, J. T. Loessberg-Zahl, B. Mei, W. Olthuis, A. van den Berg, *Sens. Actuators B* **2021**, *334*.
[74] A. Moya, M. Ortega-Ribera, X. Guimera, E. Sowade, M. Zea, X. Illa, E. Ramon, R. Villa, J. Gracia-Sancho, G. Gabriel, *Lab Chip* **2018**, *18*, 2023–2035.
[75] P. Shah, J. V. Fritz, E. Glaab, M. S. Desai, K. Greenhalgh, A. Frachet, M. Niegowska, M. Estes, C. Jager, C. Seguin-Devaux, F. Zenhausern, P. Wilmes, *Nat. Commun.* **2016**, *7*, 11535.
[76] K. Rennert, S. Steinborn, M. Groger, B. Ungerbock, A. M. Jank, J. Ehgartner, S. Nietzsche, J. Dinger, M. Kiehntopf, H. Funke, F. T. Peters, A. Lupp, C. Gartner, T. Mayr, M. Bauer, O. Huber, A. S. Mosig, *Biomaterials* **2015**, *71*, 119–131.
[77] S. A. Mousavi Shaegh, F. De Ferrari, Y. S. Zhang, M. Nabavinia, N. Binth Mohammad, J. Ryan, A. Pourmand, E. Laukaitis, R. Banan Sadeghian, A. Nadhman, S. R. Shin, A. S. Nezhad, A. Khademhosseini, M. R. Dokmeci, *Biomicrofluidics* **2016**, *10*, 044111.
[78] M. A. U. Khalid, Y. S. Kim, M. Ali, B. G. Lee, Y. J. Cho, K. H. Choi, *Biochem. Eng. J.* **2020**, *155*.
[79] Z. Liao, Y. Zhang, Y. Li, Y. Miao, S. Gao, F. Lin, Y. Deng, L. Geng, *Biosens. Bioelectron.* **2019**, *126*, 697–706.
[80] N. M. Pires, T. Dong, U. Hanke, N. Hoivik, *Sensors* **2014**, *14*, 15458–15479.
[81] Z. C. Hu, B. J. Deibert, J. Li, *Chem. Soc. Rev.* **2014**, *43*, 5815–5840.
[82] X. D. Wang, O. S. Wolfbeis, *Chem. Soc. Rev.* **2014**, *43*, 3666–3761.
[83] S. M. Borisov, O. S. Wolfbeis, *Chem. Rev.* **2008**, *108*, 423–461.
[84] S. Perottoni, N. G. B. Neto, C. Di Nitto, R. I. Dmitriev, M. T. Raimondi, M. G. Monaghan, *Lab Chip* **2021**, *21*, 1395–1408.
[85] X. K. Li, M. Soler, C. I. Ozdemir, A. Belushkin, F. Yesilkoy, H. Altug, *Lab Chip* **2017**, *17*, 2208–2217.
[86] J. F. Lee, G. M. Stovall, A. D. Ellington, *Curr. Opin. Chem. Biol.* **2006**, *10*, 282–289.
[87] X. X. Lin, Q. S. Chen, W. Liu, J. Zhang, S. Q. Wang, Z. X. Lin, J. M. Lin, *Sci. Rep.* **2015**, *5*.
[88] J. W. Grate, O. B. Egorov, M. J. O'Hara, T. A. Devol, *Chem. Rev.* **2008**, *108*, 543–562.
[89] S. X. Xia, X. Zhai, Y. Huang, J. Q. Liu, L. L. Wang, S. C. Wen, *J. Lightwave Technol.* **2017**, *35*, 4553–4558.
[90] J. J. Liu, M. Jalali, S. Mahshid, S. Wachsmann-Hogiu, *Analyst* **2020**, *145*, 364–384.
[91] L. Zeni, C. Perri, N. Cennamo, F. Arcadio, G. D'Agostino, M. Salmona, M. Beeg, M. Gobbi, *Sci. Rep.* **2020**, *10*.
[92] P. V. T. K. L. Wasewar, in *Environmental Applications of Microbial Nanotechnology* (Ed.: V. K. Pardeep Singh, Mansi Bakshi, Chaudhery Mustansar Hussain, Mika Sillanpää), Elsevier, **2023**, pp. 43–64.
[93] R. Kumar, S. Pal, Y. K. Prajapati, J. P. Saini, *Silicon-Neth* **2021**, *13*, 1887–1894.
[94] G. Zanchetta, R. Lanfranco, F. Giavazzi, T. Bellini, M. Buscaglia, *Nanophotonics-Berlin* **2017**, *6*, 627–645.
[95] X. Li, Y. L. Lu, Q. J. Liu, *Talanta* **2021**, *235*.
[96] A. Noori, S. J. Ashrafi, R. Vaez-Ghaemi, A. Hatamian-Zaremi, T. J. Webster, *Int. J. Nanomed.* **2017**, *12*, 4937–4961.
[97] M. A. Ortega, J. Rodriguez-Comas, O. Yavas, F. Velasco-Mallorqui, J. Balaguer-Trias, V. Parra, A. Novials, J. M. Servitja, R. Quidant, J. Ramon-Azcon, *Biosensors* **2021**, *11*.
[98] J. Y. Zhu, J. C. He, M. Verano, A. T. Brimmo, A. Glia, M. A. Qasaimeh, P. Y. Chen, J. O. Aleman, W. Q. Chen, *Lab Chip* **2018**, *18*, 3550–3560.
[99] M. Roy, D. Seo, S. Oh, J. W. Yang, S. Seo, *Biosens. Bioelectron.* **2017**, *88*, 130–143.
[100] J. L. Zhang, J. S. Sun, Q. Chen, J. J. Li, C. Zuo, *Sci. Rep.* **2017**, *7*.
[101] S. Moon, H. O. Keles, A. Ozcan, A. Khademhosseini, E. Hæggstrom, D. Kuritzkes, U. Demirci, *Biosens. Bioelectron.* **2009**, *24*, 3208–3214.
[102] B. C. Buchanan, J. Y. Yoon, *Micromachines* **2022**, *13*.
[103] Z. W. Hu, X. Zhou, J. Duan, X. Q. Wu, J. M. Wu, P. C. Zhang, W. Z. Liang, J. L. Guo, H. H. Cai, P. H. Sun, H. B. Zhou, Z. J. Jiang, *Sens. Actuators B* **2021**, *334*.
[104] N. Choi, H. Dang, A. Das, M. S. Sim, I. Y. Chung, J. Choo, *Biosens. Bioelectron.* **2020**, *164*.
[105] A. F. Chrimes, K. Khoshmanesh, P. R. Stoddart, A. Mitchell, K. Kalantar-zadeh, *Chem. Soc. Rev.* **2013**, *42*, 5880–5906.
[106] R. Hunter, A. N. Sohi, Z. Khatoon, V. R. Berthiaume, E. I. Alarcon, M. Godin, H. Anis, *Sens. Actuators B* **2019**, *300*.
[107] C. Novara, A. Chiado, N. Paccotti, S. Catuogno, C. L. Esposito, G. Condorelli, V. De Franciscis, F. Geobaldo, P. Rivolo, F. Giorgis, *Faraday Discuss.* **2017**, *205*, 271–289.
[108] A. Teixeira, J. L. Paris, F. Roumani, L. Dieguez, M. Prado, B. Espina, S. Abalde-Cela, A. Garrido-Maestu, L. Rodriguez-Lorenzo, *Materials* **2020**, *13*.
[109] K. B. Shanmugasundaram, J. R. Li, A. I. Sina, A. Wuethrich, M. Trau, *Mater Adv* **2022**, *3*, 1459–1471.
[110] S. Y. Sun, J. Y. Zheng, R. H. Sun, D. Wang, G. L. Sun, X. S. Zhang, H. Y. Gong, Y. Li, M. Gao, D. W. Li, G. C. Xu, X. Liang, *Nanomaterials* **2022**, *12*.
[111] M. K. Fan, G. F. S. Andrade, A. G. Brolo, *Anal. Chim. Acta* **2020**, *1097*, 1–29.
[112] M. Muhammad, C. S. Shao, Q. Huang, *Sens. Actuators B* **2021**, *334*.
[113] Y. Liu, S. H. Wu, X. Y. Du, J. J. Sun, *Sens. Actuators B* **2021**, *338*.
[114] S. M. Meyer, C. J. Murphy, *Nanoscale* **2022**, *14*, 5214–5226.
[115] C. Gu, F. J. Shan, L. F. Zheng, Y. Zhou, J. Hu, G. J. Chen, *J. Mater. Chem. B* **2022**, *10*, 1434–1441.
[116] C. Andreou, M. R. Hoonejani, M. R. Barmi, M. Moskovits, C. D. Meinhart, *ACS Nano* **2013**, *7*, 7157–7164.
[117] N. D. Kline, A. Tripathi, R. Mirsafavi, I. Pardoe, M. Moskovits, C. Meinhart, J. A. Guicheteau, S. D. Christesen, A. W. Fountain, *Anal. Chem.* **2016**, *88*, 10513–10522.
[118] A. Pallaoro, M. R. Hoonejani, G. B. Braun, C. D. Meinhart, M. Moskovits, *ACS Nano* **2015**, *9*, 4328–4336.
[119] J. Y. Fei, L. Wu, Y. Z. Zhang, S. F. Zong, Z. Y. Wang, Y. P. Cui, *ACS Sens.* **2017**, *2*, 773–780.
[120] N. A. Owens, L. B. Laurentius, M. D. Porter, Q. Li, S. Wang, D. Chatterjee, *Appl. Spectrosc.* **2018**, *72*, 1104–1115.
[121] W. Wang, P. Y. Ma, D. Q. Song, *Luminescence* **2022**, *37*, 1822–1835.
[122] A. R. Vollertsen, A. Vivas, B. van Meer, A. van den Berg, M. Odijk, A. D. van der Meer, *Biomicrofluidics* **2021**, *15*.

Manuscript received: August 9, 2023
Revised manuscript received: November 13, 2023
Accepted manuscript online: November 15, 2023
Version of record online: November 15, 2023

REVIEW

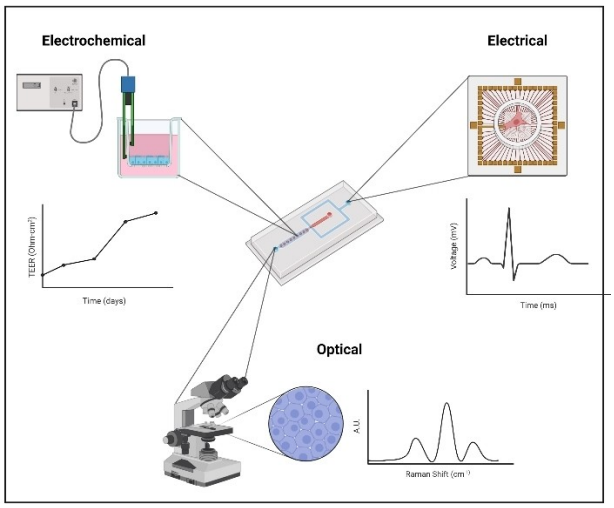

P. Tawade, Dr. M. Mastrangeli**

Integrated bio-sensing is expected to address the partly unmet need for accurate microenvironmental monitoring in organs-on-chip. This paper briefly reviews available options for integrated electrical, electrochemical, and optical sensing methods, consolidating and expanding organ-on-chip capabilities for a widening variety of applications. We spotlight recent advances and future prospects for biocompatible, non-invasive and continuous sensing techniques, and argue for the significance of highly-sensitive on-chip sensors for deepening understanding of human (patho)physiology and reproducibility of OoC technology.